Journal of Microfluidic and Nanofluidic Research

Research Article

Effect of Inlet Velocity and Voltage on the Mixing Performance of an Electroosmotic Device

Narges Jafari Ghahfarokhi[a,*], Ahmad Najafpour[b]

[a]Department of Mechanical Engineering, University of Isfahan, Isfahan, Iran

[b]Department of Mechanical Engineering, Babol Noshirvani University of Technology, Babol, Iran

ARTICLE INFO

ABSTRACT

Electroosmotic micromixers are utilized in microfluidic systems, especially in biochemical studies. This article examines an asymmetric electroosmotic micromixer to ascertain the effects of applied voltage and inlet velocity (U_{in}) on mixing index (MI) and pressure drop (Δp). It is shown that without altering Δp, the applied voltage greatly increases MI. For instance, when U_{in}= 0.2 mm/s, increasing the applied voltage from 0 to 1, 3, and 6 V improves MI by 2.31%, 2.53%, and 5.47%, respectively. MI is improved by 2.76%, 3.66%, and 8.38%, respectively, when the applied voltage is increased from 0 to 1, 3, and 6 V with U_{in}= 0.4 mm/s. MI is improved by 2.86%, 5.08%, and 11.81%, respectively, when the applied voltage is increased from 0 to 1, 3, and 6 V when U_{in}= 0.6 mm/s. MI is improved by 3.97%, 6%, and 13.22%, respectively, when the applied voltage is increased from 0 to 1, 3, and 6 V with U_{in}= 0.8 mm/s. For a given applied voltage, it is seen that Δp increases slightly when the inlet velocity is raised; also, Δp is an increasing function of the applied voltage for a given inlet velocity, despite the little increase.

1. Introduction

Small platforms known as lab-on-a-chip (LOC) devices combine laboratory operations onto a single chip, usually ranging in size from a few millimeters to square centimeters. These gadgets manipulate and examine tiny fluid quantities by utilizing microfluidics. The study of fluids at the microscale, which enables exact control over minuscule volumes of liquids, is known as microfluidics. LOCs are perfect for applications needing high-throughput analysis and low reagent use since they can handle incredibly tiny fluid volumes. DNA sequencing, medical diagnostics, and tissue engineering are just a few of the biomedical applications that employ them. They provide benefits including quicker analysis times, lower costs, and better process control. [1-3].

Mixing, pumping, and sensing are made possible by the microchannels and chambers found in microfluidic chips. Materials like silicon, glass, or polymers are used to make these chips. The technique is appropriate for use in pharmaceutical engineering, biotechnology, and patient diagnostics as it enables multiplexing and high-throughput screening. Additionally, microfluidics facilitates the development of portable point-of-care devices that improve efficiency and accessibility in medical environments. With advancements in fabrication processes, microfluidics continues to progress despite the difficulties in scaling down detection principles and the complexity of production. All things considered, microfluidics and lab-on-a-

---

* Corresponding author.

E-mail address: nargesjafari1674@gmail.com

chip technologies are revolutionizing biomedical research and diagnostics by offering small, effective, and affordable solutions [4, 5].

Because they provide effective fluid mixing at the microscale, micromixers are vital to microfluidics and its many applications in biology, chemistry, and medicine, such as drug creation and biomedical diagnostics.

Active and passive are the two general categories into which micromixers fall. Passive micromixers, on the other hand, use geometric adjustments to enhance the contact area between fluids and create chaotic advection. [6-8]. Their simplicity and minimal reagent use make them widely utilized in biological and chemical processes.

Active micromixers improve mixing by generating intricate fluid movements inside the microchannel using external energy sources [9-12].

In a contraction-expansion microchannel, AC electroosmotic mixing was investigated by Gong and Cheng [13]. The study discovered that inertia and electroosmotic forces have an impact on the creation of rotating vortices. Under higher inlet velocities, mixing quality was diminished by greater inertial force. In a 70 μm length-channel, the optimal mixing quality (0.997) was attained with a pressure drop of just 1.58 Pa at 0.2 mm/s inlet velocity and 0.1 V voltage.

The fractal concept and the width-to-length ratio of the AC electrode were combined by Lv et al. [14] to offer a three-objective optimization approach for an AC electrothermal theory-based micromixer. Temperature rise, mixing energy cost, and mixing index were the goal functions. While a surrogate model was constructed using the response surface function approach, design points were chosen using the Latin Hypercube Sampling method. The surrogate model was optimized using a multi-objective genetic algorithm, and the best set of solutions was categorized using K-means clustering. According to the results, the micromixer's safety and dependability were enhanced, with a maximum rise in the mixing index of 19.81% and a 73.16% reduction in the mixing energy cost.

In order to investigate the mixing length and efficiency of a T-junction micromixer based on AC electroosmotic flow for both Newtonian and non-Newtonian fluids, Alipanah and Ramiar offered a 3D transient single phase solver created in OpenFOAM. The impacts of factors such as the period of oscillation, conducting edges, and AC amplitude were examined, and the model and solver were verified using data from the literature. According to the study, even at high flow rates, employing conducting edges resulted in short mixing lengths and great mixing efficiency.

To investigate the effects of applied voltage and inlet velocity on MI and Δp, the current study presents an asymmetric electroosmotic micromixer (Fig. 1).

2. Governing Equations

The following are the continuity and Navier-Stokes equations that govern the mixing of two fluids in the unsteady state:

$$\nabla \cdot \vec{V} = 0 \tag{1}$$

$$\rho \left(\frac{\partial \vec{V}}{\partial t} + \vec{V} \cdot \nabla \vec{V} \right) = -\nabla P + \mu \nabla^2 \vec{V} \tag{2}$$

Here, $\vec{V}$ is the velocity vector, P is the pressure, ρ is the density, and μ is the dynamic viscosity.

The convective-diffusion transport equation is expressed as:

$$\frac{\partial c}{\partial t} + \vec{V} \cdot \nabla c = -D \nabla c \tag{3}$$

where c and D are concentration and molecular diffusion coefficient, respectively. Equation 4 is used to determine the electric potential:

$$\nabla^2 V = 0 \tag{4}$$

where V is the applied voltage. Besides, the mixing index is calculated as follows:

$$MI = \left(1 - \left(\sqrt{\frac{1}{N} \sum_{i=1}^{N} \left(\frac{c_i - \bar{c}}{\bar{c}} \right)^2} \right) \right) \times 100 \tag{5}$$

Here, c_i is the local concentration of each component and $\bar{c}$ is the average concentration. N also represents the number of grid points in the desired cross-section.
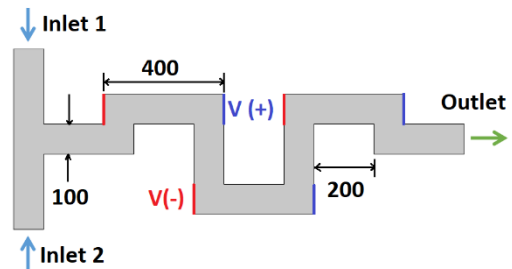

Fig. 1. Schematic of the present electroosmotic micromixer. The dimensions are in micrometers.

3. Grid Study and Validation

To perform the grid study, four grids containing 12682, 49637, 108492, and 174365 components are taken into consideration. Because the findings from the two finer grids differ very little, it is determined that the grid with 108492 components is suitable for the simulations. Fig. 2 shows the schematic form of the grid that was utilized for the simulations.
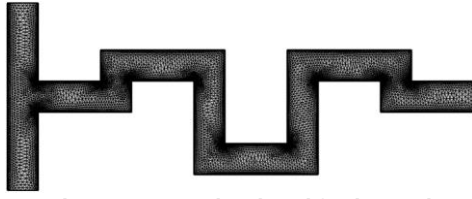
Fig. 2. The computational grid used for the simulations.

The current results are validated using the numerical results of Bahrami et al. [10]. The findings from the current numerical simulations are consistent with those published by Bahrami et al. [10], as Table 1 shows. As a result, the simulations may use the current numerical approach.

Table 1. Values of MI for various frequencies.

Frequency (Hz)	Present work	Bahrami et al. [10]
2	81.32	81.28
4	94.41	94.36
8	93.97	93.86
10	80.09	80.01

## 4. Results

One kind of active micromixer that improves fluid mixing at the microscale is an electroosmotic micromixer, which uses electric fields. An electric potential is usually applied across microelectrodes positioned within or along the walls of a microchannel in these devices. Electroosmotic flow (EOF), or fluid movement in reaction to an electric field, is induced by the electric field. This flow causes chaotic mixing and recirculation patterns by upsetting the microchannel's normally laminar flow. The zeta potential of the channel walls, the fluid's dielectric characteristics, and the intensity and arrangement of the applied electric field are some of the variables that affect the EOF.

Molecular diffusion at microscopic scales and repetitive stretching and folding of fluid components are the basic mechanisms behind efficient mixing in electroosmotic micromixers. Through the application of time-varying electric fields, these micromixers can regulate the flow and achieve excellent mixing efficiency. By producing intricate fluid movements, alternating current (AC) electroosmosis, for instance, can produce transverse flows that improve mixing. In order to optimize mixing performance, electrode location and electric field parameters are frequently optimized during the construction of electroosmotic micromixers. These systems are frequently simulated and optimized using computational models.
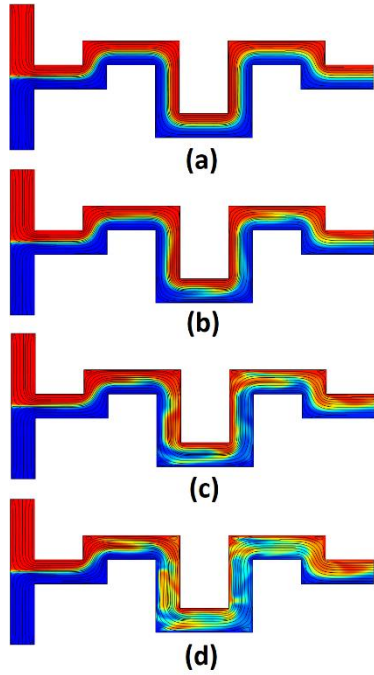
The concentration profile along the micromixer for various applied voltages is shown in Figs. 3 to 6 for U_{in} = 0.2 mm/s, 0.4 mm/s, 0.6 mm/s, and 0.8 mm/s, respectively. The mixing process is carried out by the impact of molecular diffusion when there is no electric field present. The application of the electric field improves the mixing quality by creating some vortices close to the electrodes. In other words, the formation of vortices in an electroosmotic micromixer is a crucial process for enhancing fluid mixing at the microscale. In this process, an electric field often interacts with the generated charges in the diffuse double layer near electrodes or channel walls.
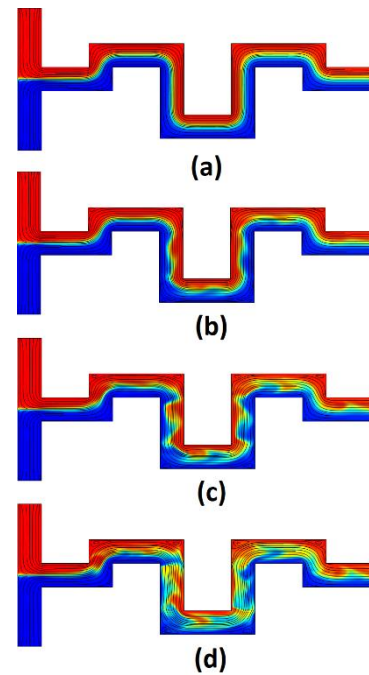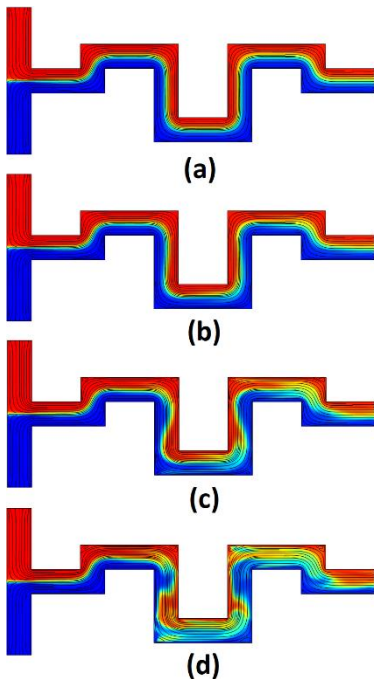

Fig. 3. Concentration contour along the micromixer for U_{in} = 0.2 mm/s when the applied voltage is: (a) 0 V, (b) 1 V, (c) 3 V, and (d) 6 V.

The amounts of MI and Δp for the several examples examined in this work are compared in Table 2. It is shown that the applied voltage greatly improves MI while not affecting Δp. When U_{in} = 0.2 mm/s, MI is improved by 2.31%, 2.53%, and 5.47% by enhancing the applied voltage from 0 to 1, 3, and 6 V, respectively. When U_{in} = 0.4 mm/s, MI is improved by 2.76%, 3.66%, and 8.38% by enhancing the applied voltage from 0 to 1, 3, and 6 V, respectively. When U_{in} = 0.6 mm/s, MI is improved by 2.86%, 5.08%, and 11.81% by enhancing the applied voltage from 0 to 1, 3, and 6 V, respectively. When U_{in} = 0.8 mm/s, MI is improved by 3.97%, 6%, and 13.22% by enhancing the applied voltage from 0 to 1, 3, and 6 V, respectively. It is observed that Δp increases slightly when the inlet velocity is enhanced for a given applied voltage. Additionally, Δp is an increasing function of the applied voltage for a specific inlet velocity, although the increase is relatively small.
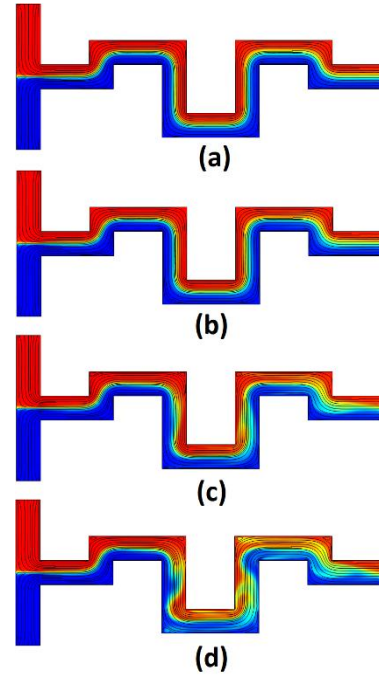
Fig. 4. Concentration contour along the micromixer for U_{in} = 0.4 mm/s when the applied voltage is: (a) 0 V, (b) 1 V, (c) 3 V, and (d) 6 V.

Fig. 6. Concentration contour along the micromixer for U_{in} = 0.8 mm/s when the applied voltage is: (a) 0 V, (b) 1 V, (c) 3 V, and (d) 6 V.

Table 2. MI and Δp values for different inlet velocities and applied voltages.

Voltage (V)	U_{in} (mm/s)	Δp (Pa)	MI (%)
0	0.2	1.06	63.42
	0.4	2.12	65.16
	0.6	3.18	65.28
	0.8	4.24	65.47
1	0.2	1.06	64.89
	0.4	2.12	66.96
	0.6	3.18	67.15
	0.8	4.24	68.07
3	0.2	1.08	65.03
	0.4	2.13	67.55
	0.6	3.19	68.60
	0.8	4.26	69.40
6	0.2	1.09	66.89
	0.4	2.15	70.62
	0.6	3.21	72.99
	0.8	4.28	74.73

Fig. 5. Concentration contour along the micromixer for U_{in} = 0.6 mm/s when the applied voltage is: (a) 0 V, (b) 1 V, (c) 3 V, and (d) 6 V.

5. Conclusions

To determine how applied voltage and inlet velocity affect MI and Δp, this work investigates an asymmetric electroosmotic micromixer. It is demonstrated that the applied voltage significantly enhances MI without changing Δp. When U_{in} = 0.2 mm/s, MI is enhanced by 2.31%, 2.53%, and 5.47% by boosting the applied voltage from 0 to 1, 3, and 6 V, respectively. When U_{in} = 0.4 mm/s, increasing the applied voltage from 0 to 1, 3, and 6 V improves MI by 2.76%, 3.66%, and 8.38%, respectively. When U_{in} = 0.6 mm/s, increasing the applied voltage from 0 to 1, 3, and 6 V improves MI by 2.86%, 5.08%, and 11.81%, respectively; when U_{in} = 0.8 mm/s, increasing the applied voltage from 0 to 1, 3, and 6 V improves MI by 3.97%, 6%, and

13.22%, respectively. It is noted that Δp increases slightly when the inlet velocity is increased for a given applied voltage; additionally, Δp is an increasing function of the applied voltage for a particular inlet velocity even though the increase is minimal.

References

[1] Bayareh, M., Nazemi Ashani, M., Usefian, A., 2020. Active and passive micromixers: A comprehensive review, Chem. Eng. Process.: Process Intensif., 147, p. 10777. https://doi.org/10.1016/j.cep.2019.10777.

[2] Bayareh, M., 2022. Active cell capturing for organ-on-a-chip systems: a review, Biomedical Engineering, 67, pp. 443-459. 10.1515/bmt-2022-0232.

[3] Han, W., Li, W., Zhang, H., 2024. A comprehensive review on the fundamental principles, innovative designs, and multidisciplinary applications of micromixers, Physics of Fluids, 36(10), p. 101306.

[4] Cai, G., Xue, L., Zhang, H., Lin, J., 2017. A Review on Micromixers, Micromachines, 8(9), p. 274

[5] Jafari Ghahfarokhi, N., Bayareh, M., Nourbakhsh, A., Baghoolizadeh, M., 2024. Optimization of a novel micromixer with fan-shaped obstacles, Chem. Pap., 78, pp. 4201-4210. https://doi.org/10.1007/s11696-024-03380-y.

[6] Bahrami, D., Bayareh, M., 2022. Impacts of channel wall twisting on the mixing enhancement of a novel spiral micromixer, Chem. Pap., 76, pp. 465–476. https://doi.org/10.1007/s11696-021-01876-5.

[7] Babaie, Z., Bahrami, D., Bayareh, M., 2022. Investigation of a novel serpentine micromixer based on Dean flow and separation vortices, Meccanica, 57, pp. 73–86. https://doi.org/10.1007/s11012-021-01465-6.

[8] Usefian, A., Bayareh, M., 2020. Numerical and experimental investigation of an efficient convergent–divergent micromixer, Meccanica, 55, pp. 1025–1035. https://doi.org/10.1007/s11012-020-01142-0.

[9] Bahrami, D., Ahmadi Nadooshan, A., Bayareh, M., 2021. Effect of non-uniform magnetic field on mixing index of a sinusoidal micromixer, Korean J. Chem. Eng., 39, pp. 316–327. https://doi.org/10.1007/s11814-021-0932-zc.

[10] Bahrami, D., Bayareh, M., Usefian, A., 2023. Effect of fin-shaped electrodes on flow mixing and pressure drop in an electroosmotic micromixer, Iranian Journal of Chemistry and Chemical Engineering, 42(1), pp. 208-221. 10.30492/ijcce.2022.544521.5055

[11] Ghorbani Kharaji, Z., Bayareh, M., Kalantar, V., 2021. A review on acoustic field-driven micromixers, Int. J. Chem. React. Eng., 19, pp. 553-569. https://doi.org/10.1515/ijcre-2020-0188.

[12] Ghorbani Kharaji, Z., Kalantar, V., Bayareh, M., 2022. Acoustic sharp-edge-based micromixer: a numerical study, Chem. Pap., 76, pp. 1721–1738. https://doi.org/10.1007/s11696-021-01994-0.

[13] Gong, Y., Cheng, X., 2023. Numerical investigation of electroosmotic mixing in a contraction–expansion microchannel, Chemical Engineering and Processing - Process Intensification, 192, p. 109492.

[14] Lv, H., Chen, X, Li, X., Ma, Y., 2022. Dengying Zhang, Finding the optimal design of a Cantor fractal-based AC electric micromixer with film heating sheet by a three-objective optimization approach, International Communications in Heat and Mass Transfer, 131, p. 105867.

[15] Alipanah, M., Ramiar, A., 2017. High efficiency micromixing technique using periodic induced charge electroosmotic flow: A numerical study, Colloids and Surfaces A: Physicochemical and Engineering Aspects, 524, pp. 53-65.